

Si based Waveguide and Surface Plasmon Sensors

Peter Debackere, Dirk Taillaert, Katrien De Vos, Stijn Scheerlinck, Peter Bienstman and Roel Baets

Ghent University - Imec
Department of Information Technology
Sint-Pietersnieuwstraat 41
9000, Gent, Belgium

ABSTRACT

Silicon-on-Insulator (SOI) is a very interesting material system for highly integrated photonic circuits. The high refractive index contrast allows photonic waveguides and waveguide components with submicron dimensions to guide, bend and control light on a very small scale so that various functions can be integrated on a chip. Moreover, SOI offers a flexible platform for integration with surface plasmon based components which in turn allows for even higher levels of miniaturization. Key property of both waveguide types is the mode distribution of the guided modes: a high portion of the light is concentrated outside of the core material, thus making them suitable for sensitive detection of environmental changes.

We illustrate chemical and label-free molecular biosensing with SOI microring resonator components. In these microring resonator sensors, the shift of the resonance wavelength is measured. A ring of radius 5 micron is capable of detecting specific biomolecular interaction between the high affinity protein couple avidin/biotin down to a few ng/ml avidin concentration. We describe the integration of surface plasmon waveguides with SOI waveguides and discuss the principle of a highly sensitive and compact surface plasmon interferometric sensor suitable for biosensing. The device is two orders of magnitude smaller than current integrated SPR sensors, and has a highly customizable behavior. We obtain a theoretical limit of detection of 10^{-6} RIU for a component of length $10 \mu m$. We address material issues and transduction principles for these types of sensors.

Besides in chemical sensors, the SOI microring resonators can also be used in physical sensors. We demonstrate a strain sensor in which the shift of the resonance wavelength is caused by mechanical strain. We have experimentally characterized the strain sensors by performing a bending test.

Keywords: SOI, Integrated Biosensors, Strain Sensors, Ring Resonators, Surface Plasmons

1. INTRODUCTION

Driven by the vision of a laboratory on a chip and its impact in numerous applications such as detection, biosensing, kinetic and binding studies and point-of-care diagnostics, extensive work has been done to miniaturize sensors able to detect biological substances. The most straightforward approach to meet the requirements for high-level integration and high-throughput fabrication is using the Silicon-on-Insulator material system. This material system has several advantages that make it a viable candidate for integrating sensing functionality on a chip.¹

From a physical point of view the largest advantage is the high index contrast which allows photonic waveguides and waveguide components with submicron dimensions to guide, bend and control light on a very small scale. The high confinement and field enhancement brought by high index contrast can be exploited to build waveguide sensors in which the electromagnetic fields propagating through the device are altered due to the presence of adsorbed biomolecular layers on the surface of these waveguides. High index contrast also has enormous merits for microcavities, which undoubtedly can be considered to be one of the most important generic components for passive and active functions. High index contrast is the key to achieve microcavities with small

Send correspondence to Peter Debackere,
E-mail: Peter.Debackere@intec.UGent.be

cavity volume and high cavity quality factor. Because the resonance wavelength is strongly dependent on the effective index, these microring resonators can be used as sensor elements.²

From a technological viewpoint the advantages of Silicon-on-Insulator are even larger. Due to the CMOS industry silicon technology has reached a level of maturity that outperforms any other plane chip manufacturing technique by several orders of magnitude in terms of performance, reproducibility and throughput. All current fabrication techniques are compatible with CMOS frontend fabrication methods, all our devices have been fabricated using Deep-UV Lithography.

There are also strong economic arguments supporting the use of Silicon-on-Insulator for integrating nanophotonics structures and devices. Nanophotonic IC are fabricated with wafer scale-processes which means that a wafer can contain an enormous amount of structures. Combined with the fact that large SOI wafers are commercially available at a relatively moderate cost, this means that the price per chip can be very low. This is a significant advantage when producing sensors since one can even choose to use disposable chips.

Although the above stated advantages of Silicon-on-Insulator are quite obvious the use of this material system for sensing applications is quite new. However, we believe that SOI can miniaturize the sensor world much in the same way that SOI has miniaturized the photonics world.

In this paper we will focus on two very different domains in which miniaturized sensing applications are needed.

The first domain is that of biotechnology related sensing. To detect biological molecules, most current detection systems use antibodies that are labeled using radioactivity, enzymes or fluorescence. When such a labeled molecule binds to a surface, its presence can be detected using straightforward luminometry, fluorimetry, spectrometry, radiometry or confocal microscopy. However, such an approach is far from ideal: labeling biomolecules is an additional step which inevitably complicates the technique and reduces its versatility. Moreover, it is not trivial to perform a reliable absolute measurement using such an approach, since the binding of the label to the biomolecule is not always equally efficient and depends on environmental factors. It would be much more elegant to detect the presence of biomolecules directly, i.e. without an intermediate labeling step. We propose two different systems to integrate a label-free biosensor in Silicon-on-Insulator. The first method makes use of ring-resonators by monitoring the shift in resonance wavelength as biomolecules adsorb to the surface of the waveguides. The second method makes use of surface-plasmon interference by integrating a gold layer into a silicon waveguide.

The second domain in which sensors are being developed is that of strain-gages used in mechanics research and structural-health monitoring. A well known optical strain sensor is a Fiber Bragg Grating. However, a FBG can measure strain only in one direction and is several centimeters long. We are developing a miniaturized optical strain sensor that can measure strain in different in-plane directions. Compared to traditional electrical strain gages, optical strain sensors have some advantages. They are immune to electromagnetic interference and are suitable for long term measurements. Because the resonance wavelength is only dependent on the strain and temperature, the sensor provides an absolute measurement (if the temperature effects are compensated for). Thanks to the use of SOI, the bend radius of the ring resonators can be small and consequently the free spectral range can be quite large (tens of nanometers). The large FSR allows to put several ring resonators or sensors in series using simple wavelength multiplexing.

2. LABEL-FREE BIOSENSOR: RINGRESONATOR

Due to an enhanced light-matter interaction, the sensitivity of microcavity resonators can be very high, while the dimensions of the device can be quite small. The SOI material system allows the production of submicron sized cavities with very high quality factors.

2.1. Theory

When light couples to a microring resonator, whispering gallery modes occur when the wavelength satisfies

$$\lambda = \frac{n_{eff}L}{m}, m = 1, 2, \dots, \quad (1)$$

L being the circumference. Due to this resonance the transmission spectrum will exhibit a very sharp drop for this specific wavelength. The resonance wavelength is very sensitive to changes of the effective index, which on its turn is very sensitive to changes of the refractive index of the surrounding medium. The resonance wavelength shift that occurs when the dielectrical surroundings of a microring cavity are changed, is used for sensing.²

There are two distinct ways in which such a device can be used for sensing application. The first method is to use a monochromatic input mode and monitor the output power as a function of the refractive index of the sample. This detection approach is commonly called ‘intensity measurement mode’.³ The second mode of operation uses a broadband input mode and as a function of the refractive index of the sample medium we monitor the position of the spectral minima in the transmission curve. This approach has been called ‘wavelength interrogation mode’ in the literature.³ While the latter method is the most sensitive one, the former allows for real time interaction registration, but the detectable amount of analyte is limited.

A schematic view of the ringresonator integrated in a measurement setup with a flow cell is presented in figure 1, the inset in this figure shows an SEM picture taken of an actual fabricated ring. Figure 2 depicts a typical transmission spectrum of such a structure.

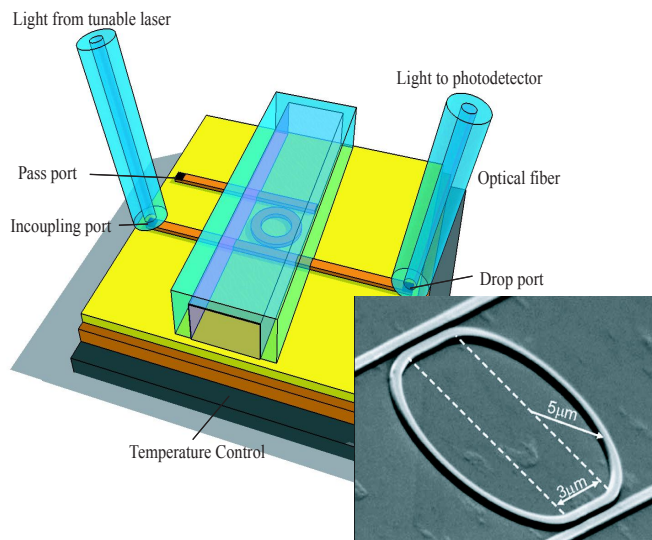


Figure 1: Schematic illustration of the measurement setup. The setup consists of a ringresonator which is integrated with a flow cell. The inset shows an SEM picture of a fabricated ring resonator.

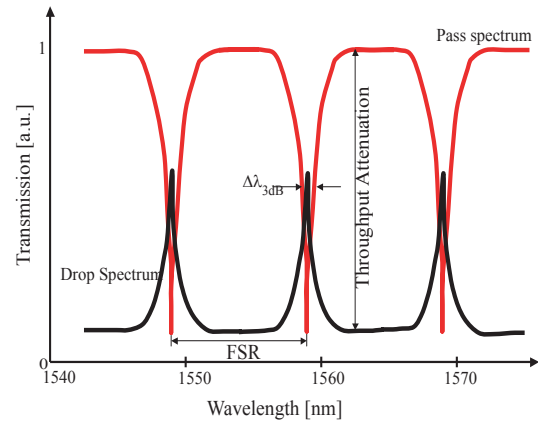


Figure 2: Typical transmission spectrum of a ring resonator

In both measurement methods the device’s sensitivity increases with increasing quality factors of the cavity, which is a measure for the ‘narrowness’ of the peaks^{4, 5}

$$Q = \frac{\lambda_{res}}{\Delta\lambda_{3dB}} \quad (2)$$

To optimize the Q factor both coupling and optical losses are minimized. Coupling losses can be reduced by increasing the gap between in- and outcoupling waveguides and the resonator. Optical losses can be minimized by choosing the optimal bend radius and by fabricating our structures using Deep-UV lithography.¹

2.2. Measurements: Bulk Refractive Index

Microring cavities of 5 micron radius with Q-factors over 20000 have been measured. In order to characterize the sensor’s sensitivity for bulk refractive index changes, liquids with varying refractive indices (aqueous solutions of *NaCl*) were flown across the ring resonator. We have measured a shift in resonance wavelength of 70 nm/RIU (Refractive Index Unit), see figure 3. A minimal detectable wavelength shift of 7.5 pm, a tenth of the peak broadness, thus corresponds with a minimal detectable refractive index change of 10⁻⁴.

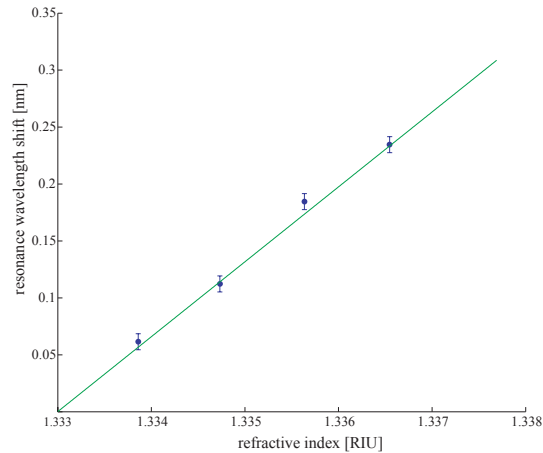


Figure 3: Resonance wavelength shift for bulk refractive index sensing with a SOI microring resonator.

2.3. Measurements: Surface Sensing of Biotin/Avidin

For proof-of-principle biosensing of protein interaction we use the high affinity couple avidin/biotin ($K_a = 10^{15} M^{-1}$). To provide a suitable biointerface between the transducer element and the biological medium the silicon surface is chemically modified (silanized). Biotin has been immobilized on an aminofunctionalized silicon surface and the biotinylated surface was then exposed to an avidin concentration to allow the complex formation. The modified surface is chemically and morphologically homogeneous, provides immobilization of the biomolecule (avidin) and prevents nonspecific adsorption.

The resonance wavelength shift after biotin/avidin interaction is depicted in figure 4, the reference level is the resonance wavelength when the sensor is immersed in Phosphate Buffer Solution (PBS). In contrast to bulk refractive index sensing, no linear curve is observed but the shift saturates for high avidin concentrations, proving this is a surface modification measurement. For low avidin concentrations the response corresponds to the concentration. The detection limit, for a 7.5 pm wavelength shift, is 50 ng/ml, which compares well to commercially available biosensing tools.

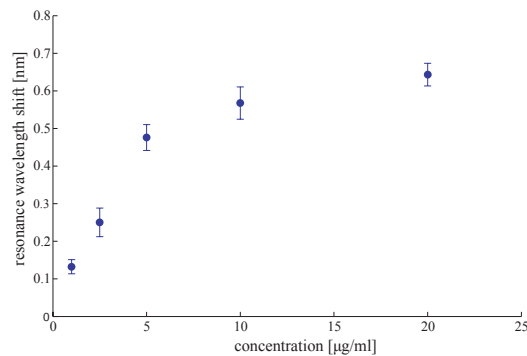


Figure 4: Quantitative avidin-biotin interaction detection with a SOI microring resonator.

3. LABEL-FREE BIOSENSOR: SURFACE PLASMON INTERFERENCE

Surface Plasmon Resonance (SPR) sensors are commercially available nowadays and provide a label-free biosensing platform. Due to these devices, the biochemistry in order to functionalize gold layers to detect different

kinds of biological substances is quite mature by now. However, the integration of surface-plasmon waveguide structures in Silicon-on-Insulator is not that straightforward.

A high index contrast material system puts fundamental limits to the resonant excitation of surface plasmons at a gold-water surface. Phase-matching of guided waveguide modes with surface plasmon modes can be obtained, but only for modes with an effective index that is much lower than the refractive index of the waveguide. Moreover, the operating spectral range of such a device will be limited and set by the conditions for phase-matching, as is the case in conventional SPR waveguide sensors. The key to the solution lies in the fact that we no longer make use of the phase-matched surface plasmon resonance but use the interference between two surface plasmon modes to sense refractive index changes.

3.1. Theory

Using interference as a means to detect refractive index changes is not new, and integrated sensors using this principle have been realized in low-index⁶ and high-index material systems.⁷ Their working principle is based on the fact that refractive index variations induce a phase-shift in one of the arms of the Mach-Zehnder interferometer (MZI), this phase-shift results in an intensity variation in the output waveguide.

$$I \propto [1 + V \cos(\Delta\phi)] \quad (3)$$

where $\Delta\phi = (\phi_r - \phi_s)$ is the phase shift between guided modes in the sensing arm and the reference arm. The visibility factor (V) gives the contrast between the maximum and the minimum transmitted intensity and depends on the coupling factor of the divisor and the propagation losses of guided modes in the interferometer arms.

The same principles can be applied to a surface plasmon interferometer. A sketch of our device is depicted in Fig. 5. The interferometer consists of a gold layer (refractive index taken from⁸) embedded into the silicon membrane ($n = 3.45$) on top of a supporting silica layer ($n = 1.45$), all dimensions and length scales are depicted in the figure. The high degree of asymmetry associated with the gold layer (top interface $n \propto 1.33$, bottom interface $n \propto 3.45$) assures that the surface plasmon modes associated with the upper and lower of the metal-dielectric interfaces will never be able to couple, their wavevectors differ too much. So the gold layer possesses two distinct surface-plasmon modes which propagate through the structure without influencing each-other. Exciting these modes is done by end-fire coupling from a regular SOI waveguide with the transverse-magnetic ground mode.^{9,10} Two independently propagating surface plasmon modes are excited at the beginning of the gold layer, they propagate independently through the structure, the phase of the top surface plasmon mode is influenced by the refractive index of the environment, while the phase of the bottom surface plasmon mode is insensitive to any refractive index changes. At the end of the gold layer both surface plasmon mode excite the ground mode of the SOI waveguide, depending on the relative phase of the surface plasmon modes their contributions to the ground mode will interfere constructively or destructively.¹¹

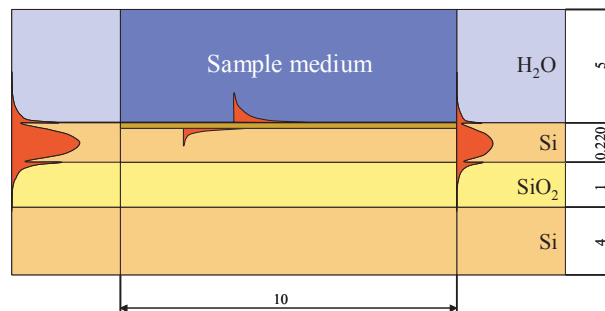


Figure 5: Schematical setup of the proposed structure, all dimensions in μm

Again there are two distinct ways in which this device can be used for sensing. We can again make use of the 'intensity measurement mode' or the 'wavelength interrogation' method.

The first interrogation method (intensity measurement mode) is illustrated in figure 6. The sensing section has a length of $10 \mu\text{m}$ and we have plotted the transmitted intensity of the fundamental TM mode of the silicon slab waveguide as a function of refractive index of the sample medium. For this simulation, we have chosen a wavelength of $1.55 \mu\text{m}$, which is in the near-infrared region and suitable for biosensing applications. The bottom part of this figure illustrates the phase difference between the top and bottom surface plasmon modes. In Fig. 7 we have simulated the response of the structure shown in Fig. 5 to a broadband incoming waveguide mode. The refractive index of the sample medium is fixed at a value of 1.33. This behavior can also be explained by comparing the phase difference between the internal and the external surface plasmon modes as can be seen in the bottom of Fig. 7.

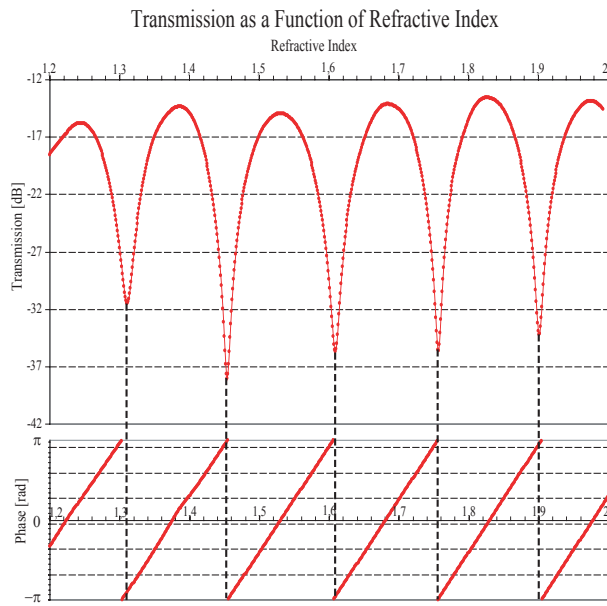


Figure 6: Transmission of the structure depicted in Fig. 5. The length of the structure is $10 \mu\text{m}$

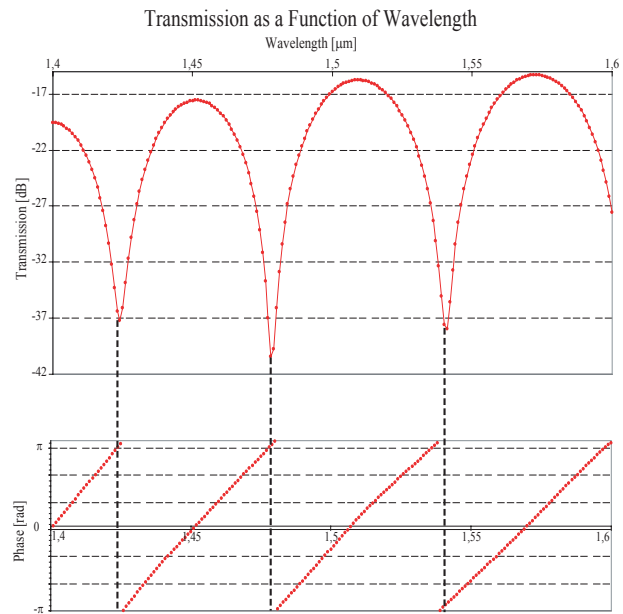


Figure 7: Transmission of the structure as a function of the wavelength

3.2. Sensitivity

Detecting refractive index changes using the intensity measurement approach yields a sensitivity for this device of $10000 \text{ dB}/\text{RIU}$. In conjunction with an optoelectronic system which can measure changes in the optical power of 0.01 dB , variations in the refractive index as small as 10^{-6} can be measured. Prism coupled SPR sensors with detection limits of 1×10^{-5} have been demonstrated³⁾, while grating coupled sensors typically have a detection limit of 5×10^{-5} RIU. Integrated sensors based on the MZI configuration display measured detection limits of 7×10^{-6} RIU,⁷ while integrated surface plasmon resonance sensors in low-index contrast material systems achieve measured values of $2000 \text{ dB}/\text{RIU}$, this corresponds to a detection limit of 5×10^{-6} RIU.¹² However, the dimensions of our device are two orders of magnitude smaller than the aforementioned devices. This means that the smallest amount of a certain molecule that can be detected will also be two orders of magnitude smaller than current integrated surface plasmon sensors.

Taking the wavelength interrogation approach, sensitivity is defined as the shift of the wavelength for which transmission is minimal as a function of the refractive index of the sample medium ($\Delta\lambda/\text{RIU}$). The value of the sensitivity can be derived from Fig. 8.

From Fig. 8 one can see that the shift of the wavelength for which transmission is minimal as a function of the refractive index of the sample medium is equal to 463.5 nm per refractive index unit. Prism based sensors have a shift of 13800 nm per refractive index unit at 850 nm ,³ and a grating based device has a value of 630 nm per refractive index unit.

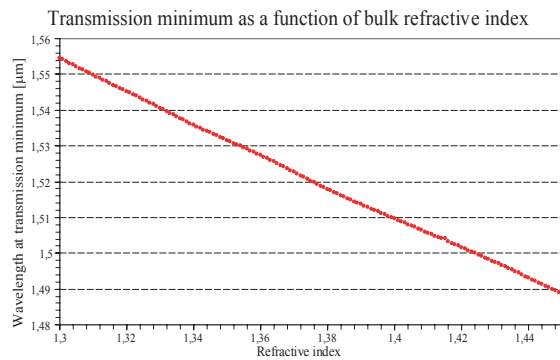


Figure 8: Shift of the wavelength for which transmission is minimal as a function of the refractive index of the sample medium

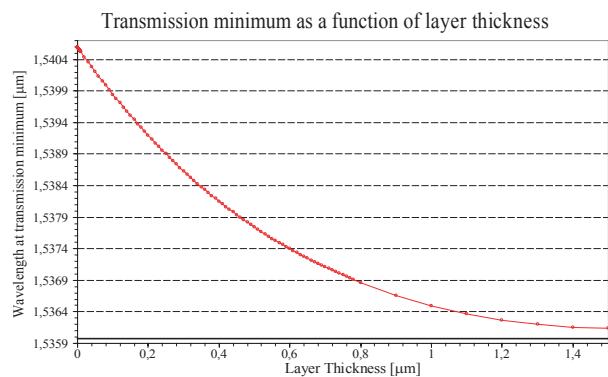


Figure 9: Shift of the wavelength for which transmission is minimal as a function of the thickness of the adsorbed layer

In order to demonstrate that our proposed device can detect very thin dielectric layers representative of thin protein layers, we have determined the shift of the wavelength for which the transmission is minimal as a function of the thickness of an adsorbed layer at the *Au*-sample medium interface. In Fig. 9 the adsorbed layer thicknesses varies from 1 to 400 *nm* and has a refractive index of 1.34. By inspection of the slope of the curve we can estimate the dependence of the peak position on the layer thickness to be approximately equal to 6 *pm/nm*. This demonstrates that our device can be used to measure layer thicknesses of adsorbed protein layers.

3.3. Fabrication

The device we have fabricated is depicted in figure 10. The device consists of broad *Si* waveguides (10 μm) of which we have etched 60 nm of *Si* using Reactive Ion Etching (RIE) over a distance of 5 μm . Using a lift-off process we have deposited 60 nm of *Au* (using thermal evaporation) where the *Si* was etched, so we end up with a 60 nm thick gold layer embedded in the *Si* waveguide. To couple light in and out of our waveguides we have used grating couplers which were optimized for *TM* polarized light. Using Focused-Ion Beam (FIB) we have made a cross-section of this device. The cross-section clearly indicates severe imperfections in the fabrication process which are mainly due to the reactive-ion-etching process. The roughness caused by this process also causes the grainy texture of the *Au* layer.

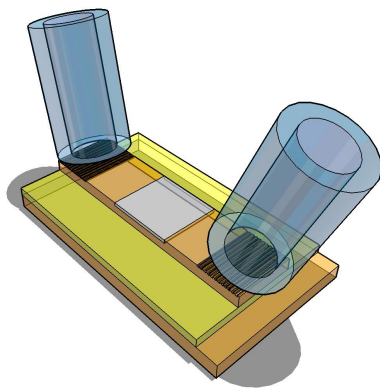


Figure 10: Schematic illustration of the fabricated device

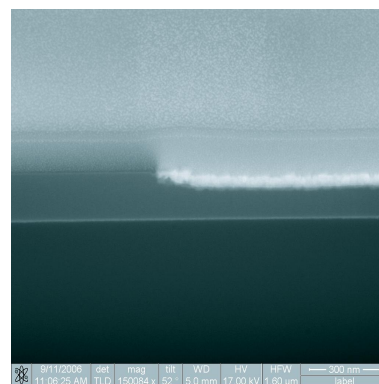


Figure 11: Cross-section of the fabricated structure made using FIB

3.4. Measurement Results

Figure 12 shows some preliminary measurement results of a sample with a *Au* length of 5 μm . The refractive index above the gold layer was 1, since the samples were measured in plain air. The difference between the three

curves is due to the fact the fill-factor of the grating couplers differs slightly. The transmission spectrum as a function of wavelength has a feature which indicates that surface plasmons are interfering in this device. However, quantitative agreement between experiment and theory has not yet been established. Several possible reasons are responsible for this discrepancy, however we expect the most important contribution to be the roughness of the etch process, which can be seen in figure 11.

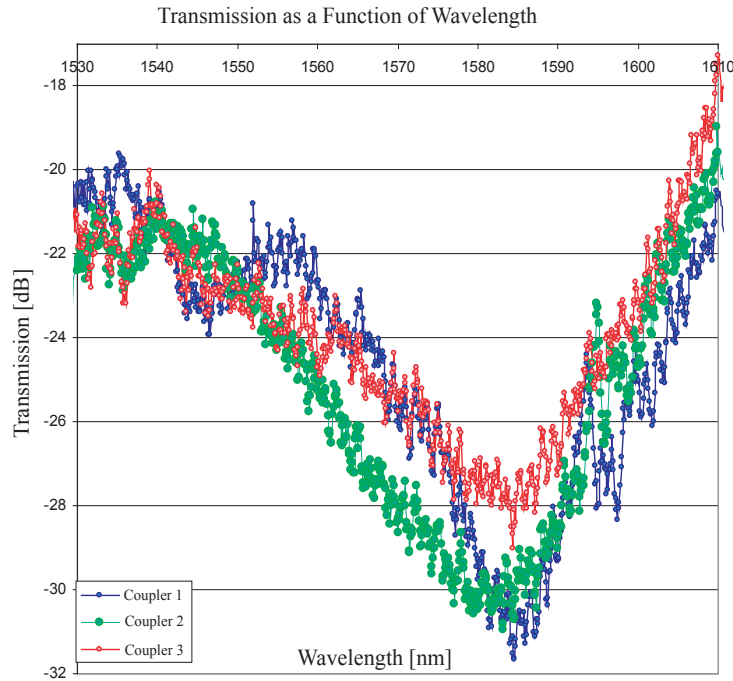


Figure 12: Preliminary measurement results for a sample with a Au length of $5 \mu m$

4. STRAIN SENSOR

Microring resonators can also be used to measure mechanical deformation or strain. Strain is defined as the relative length change $\epsilon = \Delta L/L$ and is typically expressed in microstrain ($1\mu\epsilon = 10^{-6}$). Mechanical strain will result in a shift of the resonance wavelength of the ring, which is given by

$$\frac{\Delta\lambda}{\lambda} = \frac{\Delta L}{L} + \frac{\Delta n_{\text{eff}}}{n_{\text{eff}}} \quad (4)$$

In a strainsensor, both the change of the length of the resonator and the change of the effective index (due to the photo-elastic effect) play a role. A circular ring resonator will be sensitive to strain in any in-plane direction. A racetrack resonator with straight sections will have a different sensitivity for strain in the x and y directions. A SEM picture of a circuit consisting of a circular resonator and three racetrack resonators is shown in figure 13. We will present here some preliminary experimental results on non-optimized structures. More detailed theoretical and experimental results will be published elsewhere.

Because the SOI circuits are fabricated on a thick silicon wafer, they cannot be used as a strain gage as such. The SOI circuits are transferred to a thin flexible polyimide substrate. The result is a thin flexible foil (thickness approximately $20 \mu m$) that looks similar to electrical resistance strain gages. The big difference is that the sensor on the thin foil is a SOI optical circuit instead of a metal resistor. To perform measurements,

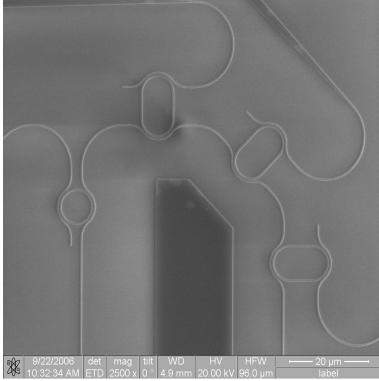


Figure 13: SEM picture of a strain sensor circuit

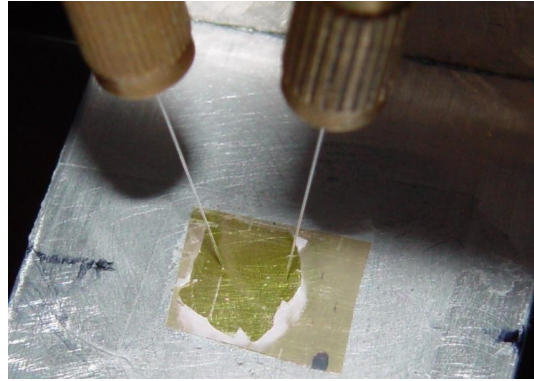


Figure 14: Photo of strain sensor bonded on Al plate

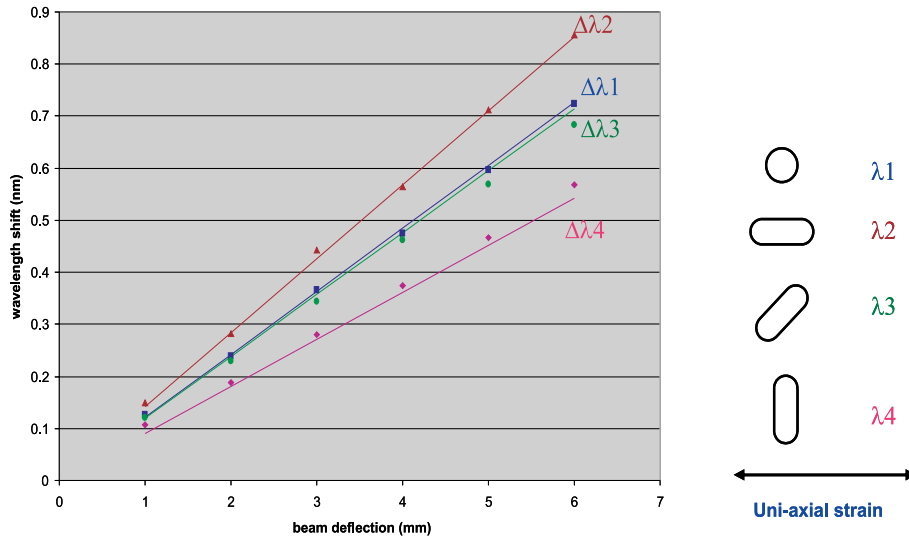


Figure 15: Measurement result of the wavelength shift.

the strain sensor is bonded to an aluminum plate. A photo of the bonded strainsensor is shown in figure 14. In our first experiments, we have bent the plate by fixing one end and moving the other end over a known distance. The bending induces tensile strain at the upper surface of the plate, that is measured by the strain sensor. The measured shift of the resonance wavelength of the resonators of figure 13, is plotted in figure 15, as a function of the deflection of the Al plate.

The sensitivity of the circular resonator is $\Delta\lambda = 0.85pm/\mu\epsilon$. In the case of the racetrack resonator, the sensitivity is $\Delta\lambda = 0.99pm/\mu\epsilon$ for strain in the longitudinal direction and $\Delta\lambda = 0.63pm/\mu\epsilon$ for strain in the transverse direction. It should be noted that the structures used are not yet optimized and that the cross sensitivity can be improved.

5. CONCLUSION

In this paper we have tried to give an overview of our sensor work in Silicon-on-Insulator. The advantages of Si in terms of high-throughput fabrication, miniaturisation and low-cost fabrication are quite obvious. Although the three different devices described here are very different in certain respect, they all benefit from the high-index contrast SOI material system.

We have demonstrated a highly miniaturized optical label-free biosensor based on an SOI microring cavity with high Q-factors. Measurement results reveal proper operation of the device, being able to detect in a

specific way avidin concentrations down to 50 ng/ml which compares favorably with commercial biosensors. The sensitivity can be improved by increasing the cavity's Q-factor and by reducing its size. Integrated in a microfluidic setup thousands of cavities can be lined up in arrays for multiparameter sensing within a few square millimeters.

The Surface-Plasmon interferometer has been described from a theoretical point of view and simulation results show that this device has a potentially high sensitivity for a very small physical footprint. Preliminary measurements indicate a proof-of-principle for this device, however fabrication methods need to be improved in order to achieve quantitative agreement between theory and experiment.

The principle of using SOI ring sensors as strain sensor has been experimentally proven.

ACKNOWLEDGMENTS

Part of work was carried out in the context of the GOA project (Ghent University), and was supported by the Belgian IAP PHOTON network and the European Union through the Network of Excellence EpixNet. Dirk Taillaert thanks the the Flemish Institute for the industrial advancement of scientific and technological Research (IWT-Vlaanderen) for a post-doctoral grant. Katrien De Vos and Stijn Scheerlinck thank the Institute for the Promotion of Innovation through Science and Technology in Flanders (IWT-Vlaanderen) for a scholarship. Peter Bienstman acknowledges the Flemish Fund for Scientific Research (FWO-Vlaanderen) for a postdoctoral fellowship.

REFERENCES

1. W. Bogaerts, R. Baets, P. Dumon, V. Wiaux, S. Beckx, T. D. B. Luyssaert, J. Van Campenhout, P. Bienstman, and D. Van Thourhout, "Nanophotonics Waveguides in Silicon-on-Insulator Fabricated with CMOS Technology," *Journal of Lightwave Technology* **23**(1), pp. 401–412, 2005.
2. R. W. Boyd and J. E. Heebner, "Sensitive Disk Resonator Photonic Biosensor," *Applied Optics* **40**, pp. 5742–5747, 2001.
3. J. Čtyrocký, J. Homola, P. Lambeck, S. Musa, H. Hoekstra, R. Harris, J. Wilkinson, B. Usievich, and N. Lyndin, "Theory and Modelling of Optical Waveguide Sensors Utilising Surface Plasmon Resonance," *Sensors and Actuators B* **54**, pp. 66–73, 1999.
4. C. Y. Chao and L. J. Guo, "Design and Optimization of Microring Resonators in Biocemical Sensing Applications," *Journal of Lightwave Technology* **24**, pp. 1395–1402, 2006.
5. E. Kriokov, J. greve, and C. Otto, "Performance of Integrated Optical Microcavities for Refractive Index and Fluorescence Sensing," *Sensors and Actuators B* **90**, pp. 58–67, 2003.
6. B. Luff, J. Wilkinson, J. Piehler, U. Hollenbach, J. Ingenhoff, and N. Fabricus, "Integrated Optical Mach-Zehnder Biosensor," *Journal of Lightwave Technology* **16**, pp. 583–592, 1998.
7. F. Prieta, Sepúlveda, A. Calle, A. Llobera, C. Domínguez, A. Abad, A. Montoya, and L. M. Lechuga, "An Integrated Optical Interferometric Nanodevice based on Silicon Technology for Biosensor Applications," *Nanotechnology* **14**, pp. 907–912, 2003.
8. E. Palik, ed., *Handbook of Optical Constants of Solids*, Academic Press, New York, 1985.
9. T. Nikolajsen, K. Leosson, I. Salkhutdinov, and B. S., "Polymer based Surface-Plasmon-Polariton Stripe Waveguides at Telecommunication Wavelengths," *Applied Physics Letters* **82**, pp. 668–670, 2003.
10. M. Hochberg, T. Baehr-Jones, C. Walker, and A. Scherer, "Integrated Plasmon and Dielectric Waveguides," *Optics Express* **12**, pp. 5481–5486, 2002.
11. P. Debackere, S. Scheerlinck, P. Bienstman, and R. Baets, "Surface Plasmon Interferometer in Silicon-on-Insulator: Novel Concept for an Integrated Biosensor," *Optics Express* **14**(16), pp. 7063–7072, 2006.
12. J. Homola, J. Čtyrocký, M. Skalský, J. Hradilová, and P. Kolářová, "A Surface Plasmon Resonance Based Integrated Optical Sensor," *Sensors and Actuators B* **38-39**, pp. 286–290, 1997.

PROCEEDINGS OF SPIE on CD-ROM

Photonics West 2007: Integrated Optoelectronic Devices

20-25 January 2007
San Jose, California, USA



Volumes 6468-6489

Single-User Edition

PROCEEDINGS OF SPIE on CD-ROM

Photonics West 2007: Integrated Optoelectronic Devices

20-25 January 2007 San Jose, California, USA Volumes 6468-6489

- 6468: Physics and Simulation of Optoelectronic Devices XV
- 6469: Optical Components and Materials IV
- 6470: Organic Photonic Materials and Devices IX
- 6471: Ultrafast Phenomena in Semiconductors and Nanostructure Materials XI and Semiconductor Photodetectors IV
- 6472: Terahertz and Gigahertz Electronics and Photonics VI
- 6473: Gallium Nitride Materials and Devices II
- 6474: Zinc Oxide Materials and Devices II
- 6475: Integrated Optics: Devices, Materials, and Technologies XI
- 6476: Optoelectronic Integrated Circuits IX
- 6477: Silicon Photonics II
- 6478: Photonics Packaging, Integration, and Interconnects VII
- 6479: Quantum Sensing and Nanophotonic Devices IV
- 6480: Photonic Crystal Materials and Devices VI
- 6481: Quantum Dots, Particles, and Nanoclusters IV
- 6482: Advanced Optical and Quantum Memories and Computing IV
- 6483: Complex Light and Optical Forces
- 6484: Vertical-Cavity Surface-Emitting Lasers XI
- 6485: Novel In-Plane Semiconductor Lasers VI
- 6486: Light-Emitting Diodes: Research, Manufacturing, and Applications XI
- 6487: Emerging Liquid Crystal Technologies II
- 6488: Practical Holography XXI: Materials and Applications
- 6489: Projection Displays XII

ISBN 9780819466259



9 0000



© SPIE
SPIE, PO Box 10, Bellingham, Washington, 98227-0010 USA
Tel: +1 360 676 3290 • Fax: +1 360 647 1445 • spie@spie.org • spie.org

9

780819466259